Convolutional Codes With a Frequency-Shift-Keying Modem

C. L. Weber[1]
Communications Systems Research Section

An analytic approximation to the probability of error per bit for the Viterbi maximum likelihood decoder of convolutional codes which employs an arbitrary modem is presented. The effect of limited path memory of the decoder on performance is determined. The method is applied in particular to the quantized binary frequency-shift-keying modem. This may be useful for entry direct links.

I. Introduction

The performance of the Viterbi maximum likelihood decoding algorithm at memory lengths where it is practical has been determined via digital simulation by Heller and Jacobs (Ref. 1) and Layland (Ref. 2). The channels that were assumed in these simulations consisted of the Binary Symmetric Channel (BSC) and the additive white Gaussian noise (AWGN) channel with a binary phase-shift-keying (PSK) modem.

We determine the performance for the Viterbi decoding algorithm with limited path memory and any encoder memory length. We are motivated since there has as yet been no analytic description of the effect of decoder memory size in the maximum likelihood decoder. This is clearly an important design consideration and a parameter which cannot be arbitrarily chosen. In addition, one clearly cannot build or simulate a decoder under all channel conditions and parameter settings.

Although the derived performance applies to any modem, emphasis is placed on the frequency-shift-keying (FSK) modem. The FSK modem is applicable, for example, in a descending atmospheric entry probe which is communicating directly to Earth where it is doubtful that a coherent RF reference phase can be maintained.

Expressions are derived which estimate the performance of a given time-invariant convolutional code for which the decoder is assumed to implement the maximum likelihood Viterbi algorithm. The results can be used to carry out a system design since the trade-off between the distance parameters of the code, the number and spacing of the quantization levels, the type of modem, and the size of the decoder memory can be analytically determined from these expressions.

[1]Consultant from the University of Southern California for the Communications Systems Research Section.

Some of these variations are presented. For example, the effect of the finite decoder memory is the addition of a term in the expression of probability of error per bit which decreases exponentially to zero as decoder memory size increases. This additional term is the dominant contribution to the probability of error for small decoder memory. The size of decoder memory at which the two terms are of the same order of magnitude is dependent on the distance parameters of the code and the signal-to-noise ratio in the modem.

Of importance in the development of the expressions for performance is an enumeration of all paths which have merged with the correct path, whose path length is less than or equal to the decoder memory. Also, an enumeration of all paths which have not merged with the correct path is required, whose path length is equal to that of the decoder memory. These enumerations are determined via transfer functions, from which approximations on the first event error probability 3 and the probability of error per bit are determined. These expressions are then applied to the binary PSK and binary FSK modem.

II. Transfer Functions for a Finite Memory Decoder

Techniques to obtain bounds on the probability of first-event error and probability of error per bit for maximum likelihood decoding have been introduced and developed by Viterbi (Ref. 3). In so doing, Viterbi introduced the transfer function of the code to enumerate the lengths of paths, the number of input *ones* corresponding to the paths, and the weight of the paths leaving the all-*zero* state and returning to the all-*zero* state at some later time. In general, the transfer function, $T(M, L, N)$ is a power series whose ijkth terms is $a_{ijk}M^iL^jN^k$, where a_{ijk} is the number of paths that pass through the modified state diagram in j branches with k input *ones* and with metric or weight i. The use of the transfer function to determine upper bounds on the bit error probability over any memoryless channel is presented in detail by Viterbi for an *infinite path memory*, maximum likelihood decoder.

Suppose now that the decoder path memory is restricted to some finite length ℓ. To now enumerate all paths which have *merged* with the all-*zero* state, again let the exponent of the dummy variable L be equal to the length of a path and the exponent of the dummy variable N be equal to the number of input *ones* corresponding to the path. For the moment we shall be concerned with the transfer function $T_\ell(L, N)$, which is to be determined so as to enumerate all paths through the modified state diagram up to length ℓ.

There is one path that leaves the all-*zero* state and returns after $K + 1$ input bits. This path is represented by NL^{K+1} since the first input bit for the path is a *one*, followed by K *zeros*. There is one path leaving the all-*zero* state and returning after $K + 2$ input bits. This path is represented by N^2L^{K+2} since it corresponds to two input *ones* followed by K *zeros*. For $K + 2 \leq \ell \leq 2K + 1$, there are $2^{\ell-(K+2)}$ paths leaving the all-*zero* state and returning after ℓ input bits. These paths have an initial input *one* corresponding to the path leaving the all-*zero* state, and there is a final input *one* followed by K *zero* input digits, so as to guarantee the return of the path to the all-*zero* state in exactly ℓ steps. The remaining $\ell - (K + 2)$ input bits can therefore be chosen arbitrarily with a distinct path corresponding to each of these input sequences. The transfer function of all paths which merge with the all-*zero* state up to length ℓ, for $K + 2 \leq \ell \leq 2K + 1$, is given by

$$T_\ell(L, N) = NL^{K+1} + N^2L^{K+2} \times \sum_{i=0}^{\ell-(K+2)} (1 + N)^i L^i \qquad K + 2 \leq \ell \leq 2K + 1 \qquad (1)$$

For $\ell > 2K + 1$, some paths then contain a sequence of K consecutive *zero* input bits among the $\ell - (K + 2)$ input bits so that the path would merge with the all-*zero* state before ℓ steps. To circumvent this, recall that the Viterbi maximum likelihood decoding algorithm rejects paths with low likelihood at the point where the path first merges with the correct path. Therefore, if the all-*zero* vector is considered to be the transmitted sequence, then only paths that return to the all-*zero* state for the first time at a given decoding step are considered. Let

$$\phi_j(N) = \begin{cases} N, & j = 1 \\ N^2(1 + N)^{j-2}, & 2 \leq j \leq K + 1 \end{cases} \qquad (2)$$

represent the enumeration of paths with information sequences of total length $j + K$, the last K input bits being zero. As the information length is increased from $j - 1$ to j, there are $\phi_{j-1}(N)$ paths for the added input being a *one* and also the same for being a *zero*. For $j > K + 1$ and $\ell > 2K + 1$, however, some of the paths of length j which result from the additional input bit being a *zero* will have K consecutive *zeros* in the $j - 2$ input bits between the initial input *one* and the final input *one*. These paths are just the paths of length j with an initial input *one* followed

by K *zeros* followed by a path of length $j-(K+1)$. The final $j-(K+1)$ path segment necessarily begins with a *one*. These paths that return to the all-*zero* state before the end of the path therefore are enumerated by $N\phi_{j-(K+1)}$ and correspond to paths that must be eliminated when enumerating all paths whose input sequence is of length exactly equal to $j+K$ through the modified state diagram. Thus for $j > K+1$, the following recursion relationship is obtained for $\phi_j(N)$:

$$\phi_j(N) = (1+N)\,\phi_{j-1}(N) - N\phi_{j-(K+1)}(N), \qquad j > K+1 \tag{3}$$

The transfer function which enumerates all paths that have merged with the all-*zero* sequence up to length ℓ is thus given by

$$T_\ell(L,N) = L^K \sum_{j=1}^{\ell-K} \phi_j(N)\,L^j, \qquad \ell > K+1 \tag{4}$$

In the special case where infinite memory is assumed, $\ell \to \infty$ and the resulting transfer function can be expressed in closed form via direct summation, namely,

$$T(L,N) \triangleq \lim_{\ell\to\infty} T_\ell(L,N) = \frac{NL^{K+1}(1-L)}{1-L(1+N)+NL^{K+1}}$$

This infinite memory transfer function has been given previously by Viterbi (Ref. 3) using a different approach.

For finite path memory ℓ input bits *must* be decoded and released to the data user after ℓ steps of decoding. Therefore, assuming the all-*zero* vector was transmitted, all paths leaving the all-*zero* state and *not returning* after ℓ input bits must be compared to determine if one of these paths has a likelihood greater than the path with the largest likelihood of all paths that have returned to the all-*zero* state at the decoding time specified. We enumerate these paths in a manner similar to that used to determine $T_\ell(L,N)$. We need to determine the transfer function

$$V_\ell(L,N) \triangleq \Psi_\ell(N)\,L^\ell \tag{5}$$

which enumerates all paths of length ℓ which leave the all-*zero* state at the outset and have not returned after ℓ input bits. Direct observation yields the fact that $\Psi_1(N) = N$, and $\Psi_\ell(N) = N(1+N)^{\ell-1}$, $\ell = 2, \cdots, K$. In order to be guaranteed that no path contains a sequence of K *zeros*, $\Psi_\ell(N)$ must satisfy the same recursion relationship as $\phi_j(N)$ in Eq. (3), namely

$$\Psi_\ell = (1+N)\,\Psi_{\ell-1}(N) - N\Psi_{\ell-(K+1)}(N)$$

for $\ell \geqq K+1$, where the initial condition $\Psi_0(N) = 1$ is needed to completely specify $\Psi_j(N)$. The recursion relationship for both types of input sequences is the same, the only difference being the sets of initial conditions.

III. Approximations to Probability of Error

Upper bounds on the probability of first event error and probability of error per bit can be obtained by direct application of the transfer functions in the previous section. These bounds are rather poor bounds, however, primarily due to the assumption that the distance between paths is set equal to the minimum distance. This assumption is quite gross, and produces tractable, but weak, upper bounds.

For short code memory length K, the complete distance structure of the code can be used to achieve tight upper bounds. In order to retain the use of only simple distance properties and improve the estimate of the probability of error, the following approximations are made to the complete distance structure of the code. To begin, consider the truncation term $V_\ell(L,N) = \Psi_\ell(N)\,L^\ell$ described above. One method to obtain an upper bound is to replace L^ℓ by $M^{d_0\ell+d_1}$, thereby replacing the distance in every path by a uniform lower bound on the minimum distance. In the above representation of the uniform lower bound, namely $d_0\ell + d_1$, we have the following definitions:

The term ℓ is the path length in branches, which in our applications will be set equal to the path length corresponding to the size of the decoder memory.

The term d_0 is the minimum average weight per branch of the code. Upper and lower bounds on d_0 for binary convolutional codes of rate $1/n$ are presented in Ref. 4. For example, $d_0 \leqq 1/2$ for rate $1/2$ codes and $d_0 \leqq 1$ for rate $1/3$ codes; these bounds are attainable by certain codes.

The term d_1 is a small bias. It represents an offset of the minimum distance from uniform growth with path length. The bias compensates for a concentration of weight over the path from the all-*zero* state to the average weight per branch cycle and compensates additionally for a concentration of weight over any part of this cycle.

With this prelude, the approach to the approximation is as follows. Various paths in the tree will have various weights. We know that for any length ℓ, the path of smallest weight is lower bounded by $d_0\ell + d_1$. The path with maximum weight is estimated by $n\ell$. We approximate all

intermediate weight paths of length ℓ by appropriate combinations of these two extreme weights as follows. Consider first the path of length $\ell = 1$. All paths into the modified state diagram begin with a *one*. We estimate the weight of the path of length equal to one branch by the transfer function $A_1(M, N)$, namely,

$$A_1(M, N) \triangleq NM^{d_0+d_1} \tag{6}$$

the N being present because all error sequences begin with a *one*, and $d_0 + d_1$ estimates the weight in this first branch. We equally well could have estimated the weight in this first branch by n; the difference will be negligible when long input sequences are considered. For $\ell = 2$, the two possible input sequences are 11 and 10. We elect to estimate the weight of the two $\ell = 2$ paths via the transfer function

$$A_2(M, N) = NM^{d_0+d_1}(NM^{d_0} + M^n) \tag{7}$$

In so doing, we assume that the added *one* in the 11 input sequence produces a small weight increase, namely d_0, and that the added *zero* in the 10 sequence produces a larger weight increase, which we estimate by n. When we add the third digit, we reserve this assumption, so that

$$A_3(M, N) = NM^{d_0+d_1}(NM^{d_0} + M^n)(NM^n + M^{d_0}) \tag{8}$$

The idea is now established; in general, therefore,

$$A_\ell(M, N) = NM^{d_0+d_1}(NM^{d_0} + M^n)^{\lceil(\ell-1)/2\rceil} \times (NM^n + M^{d_0})^{\lfloor(\ell-1)/2\rfloor} \tag{9}$$

where the $\lceil\ \rceil$ notation indicates the greatest integer in the enclosed expression and the $\lfloor\ \rfloor$ notation, the smallest integer.

This approach to averaging distances of all paths which do not return to the all-*zero* state in ℓ branches involves the same addition of extra paths as in the previous section, since no attempt has been made to remove such paths by use of the recursion relationship for $\Psi_\ell(N)$.

For small decoder memory, there exist many more non-return-to-zero paths than return-to-zero paths. The truncation term $A_\ell(M, N)$ is therefore the dominant contribution to the probability of error for small decoder memory. For large decoder memory, the effect of decoder memory decreases exponentially to zero, so that the $B(M, N)$ term to be described below for the return-to-zero paths becomes the dominant contribution to the probability of error.

By expanding $A_\ell(M, N)$ in a power series, we obtain

$$A_\ell(M, N)\Big|_{\substack{N=1\\ M^k=P_k}} = \sum_{i=0}^{\lceil(\ell-1)/2\rceil}\binom{\lceil(\ell-1)/2\rceil}{i}\sum_{j=0}^{\lfloor(\ell-1)/2\rfloor}\binom{\lfloor(\ell-1)/2\rfloor}{j}P_k \tag{10}$$

where

$$k = \lceil d_1 + d_0(1 + i + j) + n(\ell - 1 - i - j)\rceil \tag{11}$$

and where we have substituted P_k for M^k. The probability P_k is the probability of first event error between two merging paths which differ in k positions. For the approximation of probability of error per bit, we use the power series

$$\frac{\partial A_\ell(M, N)}{\partial N}\Big|_{\substack{N=1\\ M^k=P_k}} = \sum_{i=0}^{\lceil(\ell-1)/2\rceil}\binom{\lceil(\ell-1)/2\rceil}{i}\sum_{j=0}^{\lfloor(\ell-1)/2\rfloor}\binom{\lfloor(\ell-1)/2\rfloor}{j} \times \left(1 + i - j + \frac{\ell-1}{2}\right)P_k \tag{12}$$

where k is again given by Eq. (11). Equations (10) and (12) provide the contribution to the probability of first event error and probability of error per bit respectively from all paths of length ℓ which have not merged with the all-*zero* state. The length ℓ is set equal to the size of the decoder path memory.

Using similar techniques as used for the truncation term, $A_\ell(M, N)$, we now estimate the portion of the probability of error which comes from the undetected error term, which we designate as $B_\ell(M, N)$. First consider the path of length $\ell = K + 1$. The minimum distance for this path length is approximated by d_{free}. Therefore, we estimate the weight of the path of length $K + 1$ by the transfer function $B_{K+1}(M, N)$, namely,

$$B_{K+2}(M, N) \triangleq NM^{d_{\text{free}}} \simeq NM^{d_0\bar{\ell}+d_1} \tag{13}$$

where $\bar{\ell}$ is defined as follows. For a convolutional code with minimum average weight per branch d_0, bias d_1, and free distance d_{free}, there is a path length $\bar{\ell}$ such that all

paths through the modified state diagram with length greater than $\bar{l}$ have weight greater than or equal to d_{free}. This path length must satisfy $d_{\text{free}} \leq d_0 \bar{l} + d_1$, so that $\bar{l} \geq (d_{\text{free}} - d_0)/d_0$. The smallest integer $\bar{l}$ which will satisfy this requirement is therefore given by

$$\bar{l} \triangleq \left\lceil \frac{d_{\text{free}} - d_1}{d_0} \right\rceil \tag{14}$$

The weight of all paths of length $\leq K + 2$ which have returned to the all-*zero* state, the number of input *ones* in each path is given by

$$\begin{aligned} B_{K+2}(M, N) &\simeq NM^{d_0 \bar{l} + d_1} + N^2 M^{n + d_0(\bar{l}-1) + d_1} \\ &= NM^{d_0(\bar{l}-1)+d_1}(M^{d_0} + NM^n) \end{aligned} \tag{15}$$

where the path of length $K + 2$ resulting from two input *ones* has one of the branches of weight n and the rest of the branches of average weight d_0. For $l = K + 3$, there is one path resulting from two input *ones* and one path resulting from three input *ones*. Thus,

$$\left.\begin{aligned} B_{K+3}(M, N) &= NM^{d_0 \bar{l} + d_1} + 2N^2 M^{n + d_0(\bar{l}-1)+d_1} \\ &\quad + N^3 M^{2n + d_0(\bar{l}-2)+d_1} \\ B_{K+3}(M, N) &= NM^{d_0(\bar{l}-2)+d_1}(M^{d_0} + NM^n)^2 \end{aligned}\right\} \tag{16}$$

where a branch of weight n replaces a branch of weight d_0 for each input *one* into the convolutional encoder after the first *one*. Therefore, we are approximating all the intermediate weight paths of length l by combinations of the branch weights n and d_0. Continuing this procedure, for $K + 1 \leq l \leq \bar{l} + K + 1$,

$$B_l(M, N) = NM^{d_0(\bar{l}+K+1-l)+d_1}(M^{d_0} + NM^n)^{l-K-1} \tag{17}$$

The representation for $B_l(M, N)$ in Eq. (17) enumerates all paths of length less than or equal to l, when $K + 1 \leq l \leq \bar{l} + K + 1$, which have departed from the all-*zero* state at time zero, and returned at some time less than that corresponding to l branches. The reason for approximating the weights of the various paths by $B_l(M, N)$ in this manner is to force the approximation to be such that the smallest weight path at each length l, $K + 1 \leq l \leq \bar{l} + K + 1$, be equal to d_{free}.

For $l > \bar{l} + K + 1$, we know that all paths through the modified state diagram have weight greater than d_{free}, so that the above restriction need no longer be imposed. We proceed, therefore, as with $A_l(M, N)$ so that

$$B_l(M, N) = NM^{d_1}(M^{d_0} + NM^n)^{\bar{l}} \cdot \left[\sum_{k=0}^{l-(\bar{l}+K+1)} (M^{d_0} + NM^n)^{\lceil k/2 \rceil} (NM^{d_0} + N^n)^{\lfloor k/2 \rfloor} \right] \tag{18}$$

By expanding $B_l(M, N)$ in a power series as was similarly done for $A_l(M, N)$ in Eq. (10) and again making the substitution $M^r = P_r$, we obtain

$$B_l(M, N) \Big|_{\substack{N=1 \\ M^r = P_r}} = \sum_{k=0}^{l-\bar{l}-K-1} \sum_{i=0}^{\lceil (k+\bar{l})/2 \rceil} \sum_{j=0}^{\lfloor (k+\bar{l})/2 \rfloor} \binom{\lceil (k+\bar{l})/2 \rceil}{i} \binom{\lfloor (k+\bar{l})/2 \rfloor}{j} P_r \tag{19}$$

where

$$r = d_1 + d_0(i + j) + (k + \bar{l} - i - j)n \tag{20}$$

For the approximation of probability of error per bit, we use the power series

$$\frac{\partial B_l(M, N)}{\partial N} \Big|_{\substack{N=1 \\ M^r = P_r}} = \sum_{k=0}^{l-\bar{l}-K-1} \sum_{i=0}^{\lceil (k+\bar{l})/2 \rceil} \sum_{j=0}^{\lfloor (k+\bar{l})/2 \rfloor} \binom{\lceil (k+\bar{l})/2 \rceil}{i} \binom{\lfloor (k+\bar{l})/2 \rfloor}{j} (1 + j - i + \lceil (k + \bar{l})/2 \rceil) P_r \tag{21}$$

where r is given by Eq. (20).

In summary, we have approximated the probability of error per bit for a given convolutional code employing the Viterbi maximum likelihood decoder with finite decoder memory by

$$P_b \approx \left[\frac{\partial A_\ell(M,N)}{\partial N} + \frac{\partial B_\ell(M,N)}{\partial N}\right]\Bigg|_{\substack{N=1 \\ M^r = P_r}} \tag{22}$$

where

$$\partial A_\ell(M,N)/\partial N$$

is given by Eq. (12) and

$$\partial B_\ell(M,N)/\partial N$$

is given by Eq. (21). The first term in Eq. (22) represents the contribution to the probability of error per bit due to the fact the decoder has a finite memory, measured in terms of the finite path length ℓ. The second term represents the undetected error from paths with length less than or equal to that of the decoder memory, which have merged with the correct path. What remains is to evaluate P_k for the particular modem that is to be used, which is considered in the next section.

IV. First Error Probability P_k for Various Quantized Channels

The approximations of the probability of error considered above apply to any memoryless channel. In the present context, by channel we mean to include all preliminary signal processing which may take place before the data are given to the Viterbi maximum likelihood sequence decoder.

The channel of primary interest is the AWGN channel with Q-levels of quantization. A block diagram of the demodulator for the pulse-code modulation (PCM)-PSK biphase signal is shown in Fig. 1. Two different demodulators of the PCM-binary FSK signal with quantization are shown in Figs. 2 and 3. More will be said about these in the following discussion.

For simplicity, we shall assume a binary-encoded signal. Regardless of the modem used, the analog voltage of the output of the matched filter, or the difference of the outputs of two envelope detectors, is assumed to be quantized into Q equally spaced levels. This quantized output is mapped via a metric, once under the assumption the transmitted symbol represents a *one*, and once for a *zero*. The metric outputs $w_{ij}^{(0)}$ and $w_{ij}^{(1)}$ in Figs. 1–3 represent the ith symbol in the jth branch under the assumption that a 0 and 1 were transmitted respectively.

The optimal map which minimizes the probability of error is the log likelihood functional, for which $w_{ij}^{(n)}$ is analog and is given by

$$w_{ij}^{(n)} = \log P(y_{ij}|H_n), \qquad n = 0, 1 \tag{23}$$

The evaluation of the error event probability P_k is then determined by considering two code sequences, x and x', which disagree in k symbols. Assume x is the correct sequence and is the all-*zero* sequence, so that x' is *one* in each of the specified k positions. Then

$$P_k = \text{Prob}\left\{\sum_{r=1}^{k}\left[\ln P(y_r|x_r') - \ln P(y_r|x_r)\right] > 0\right\} \tag{24}$$

if the optimal log likelihood functional is used. The summation in Eq. (24) is over the k symbols in which x and x' disagree.

For ease of implementation, the log likelihood functional is quantized and mapped into the set of integers $0, \cdots, Q-1$. When the quantization levels are assumed to be equally spaced, extensive computation of the PSK modem has demonstrated that the map is sufficiently nonlinear, so that $w_{ij}^{(n)}$ is not a good approximation of $\ln P(y_r|H_n)$. The function that is the primary contributor to P_k, however, is the difference of log likelihood functionals, as indicated in Eq. (24), for the Viterbi maximum likelihood sequence decoder. The map of $\ln P(y_r|1) - \ln P(y_r|0)$ into $w_r^{(1)} - w_r^{(0)}$, for the PSK modem, is satisfactorily linear over an extensive range of equally spaced quantization levels and ratios of signal energy to noise spectral density, E_s/N_0. Examples are shown in Figs. 4 and 5. In Fig. 4, with eight equally spaced levels of 0.5, the linearity of the interior regions is almost perfect. The only deviation is in the two extreme quantization bins $(-\infty, -1.5)$ and $(1.5, \infty)$, which increase in probability as the signal-to-noise ratio E_s/N_0 increases. In Fig. 5, this becomes extensive when the size of the equal spacing is decreased to 0.25. The linearity of the interior regions predominates over all E_s/N_0 and quantization spacings.

Because of this approximate linearity as well as the simplicity which results from this approximation, most implementations of the Viterbi decoder employ equally spaced quantization levels and linear metrics. The extension to arbitrarily spaced bins is straightforward. For the PSK modem, the relationships are as shown in Table 1.

Table 1. Relationships for the PSK modem

z_{ij}	0	1	2	$\cdots$	$Q-2$	$Q-1$
$w_{ij}^{(1)}$	0	1	2	$\cdots$	$Q-2$	$Q-1$
$w_{ij}^{(0)}$	$Q-1$	$Q-2$	$Q-3$	$\cdots$	1	0

We shall adopt the following notation:

$$P(w_{ij}^{(1)} = q \,|\, x_{ij} = 1) = P_q, \qquad q = 0, \cdots, Q-1 \quad (25a)$$

so that

$$P(w_{ij}^{(1)} = q \,|\, x_{ij} = 0) = P_{Q-1-q}, \qquad q = 0, \cdots, Q-1 \quad (25b)$$

Since $w_r^{(0)} = Q - 1 - w_r^{(1)}$, we have the result that

$$P_k = \text{Prob}\left\{\sum_{r=1}^{k} w_r^{(1)} > \frac{k(Q-1)}{2} \,|\, x_r = 0\right\} \quad (26)$$

for the quantized system.

Therefore, P_k is equal to the probability that the sum of discrete, identically distributed, statistically independent random variables is greater than a threshold, where each random variable can take on the integer values $0, \cdots, Q-1$.

V. Binary FSK Modem With Quantization

If the channel degrades the signal sufficiently so that coherent tracking of the RF reference phase cannot be satisfactorily maintained, an alternative is binary FSK. This is anticipated to be the case in a descending atmospheric entry probe where an RF reference phase may not be adequately maintained. In this section the use of the quantized FSK modem is described. Configurations are suggested for the binary FSK modem, which are directly extendable to multiple-frequency-shift keying (MFSK).

The optimal choice of $M = 2^K$ in MFSK from the point of view of maximizing channel capacity or R_{comp} is given by I. Bar-David and S. Butman (Ref. 4), where it is shown that choosing $M = 2$ is not best at any signal-to-noise ratio.

The simplest way to implement a binary FSK demodulator with Q-levels of quantization is shown in Fig. 2, which we have called system A. The output of each envelope detector is sampled at the end of each symbol time. Perfect synchronization is assumed. Under the assumption, for example, that frequency f_1 was transmitted over the channel during a given symbol time, the probability density function (PDF) of r_1 in Fig. 2 will be Rician distributed, and r_0 will be Rayleigh distributed. These analog samples are differenced and quantized into one of Q levels or bins. This output $\{z_{ij}\}$ is then mapped into a metric under each of the two hypotheses. The simplest metric is linear and the question immediately arises as to how representative this metric is of the log likelihood.

The envelope detectors are assumed to output r_1^2 and r_0^2 respectively, so that in system A,

$$y \triangleq y_{ij} = r_1^2 - r_0^2 \quad (27)$$

The envelope detector outputs are assumed to be appropriately normalized so that

$$p(r_0) = r_0 \exp\left(-\frac{1}{2} r_0^2\right), \qquad \text{Rayleigh}, \; r_0 \geqq 0$$

and

$$p(r_1) = r_1 \exp\left[-\frac{1}{2}(r_1^2 + \lambda^2)\right] I_0(\lambda r_1), \qquad \text{Rician}, \; r_1 \geqq 0$$

where $\lambda^2 = 2E_s/N_0$, $E_s = ST_s$ being the symbol energy.

The cumulative density of y under the assumption that H_1 is true can be shown to be

$$F(y) = \begin{cases} \frac{1}{2}\exp\left(-\frac{\lambda^2}{4} + \frac{y}{2}\right), & y \leqq 0 \\ 1 - Q(\lambda, \sqrt{y}) + \frac{1}{2}\exp\left(-\frac{\lambda^2}{4} + \frac{y}{2}\right) \\ \quad \times Q(\lambda/\sqrt{2}, \sqrt{2y}), & y \geqq 0 \end{cases} \quad (28)$$

where $Q(\alpha, \beta)$ is the Marcum Q-function (Ref. 5).

As in PSK, we assume y is quantized with equally spaced levels and the metric maps are linear as in Table 1. How representative this metric is of the difference of log likelihood functionals has been determined for binary FSK using $F(y)$ in Eq. (28). Examples are shown in Figs. 6 and 7. Examination of the Rayleigh and Rician PDFs indicates that a reasonable choice for the size of equally spaced quantization interval is given by the point

where the two PDFs intersect.[2] In the case $Q = 8$, two equally spaced intervals are placed between the origin and the point of intersection. For a given λ^2, the quantization interval is then given by that Δ which satisfies

$$\exp(\lambda^2/2) = I_0(\lambda\sqrt{Q\Delta/2}), \qquad Q = 8 \tag{29}$$

In Fig. 6, the Δ corresponding to Eq. (29) was used. At all signal-to-noise ratios considered, the difference of the log likelihoods of the probability of being in a given quantization region under H_1 and H_0 is quite linear, particularly at $E_s/N_0 = 2$ dB. Thus choosing the quantization interval based on Eq. (29) is a satisfactory rule of thumb. This assumes, of course, *a priori* knowledge of E_s/N_0. It is also reasonable to expect this choice of Δ to be very close to that Δ which will maximize the capacity of the quantized channel.

In Fig. 7, the quantization interval is fixed at $\Delta = 1$, and the difference of the log likelihoods is shown for different E_s/N_0. It is noted that $\Delta = 1$ is too small a quantization interval at $E_s/N_0 = 2$ dB, so poor in fact that the difference of the log likelihoods is no longer monotonic. Also, binary FSK does not have the satisfying property that is consistent with binary PSK, namely, of being linear over the interior quantization regions over a wide range of Δ and E_s/N_0.

In a given application, it is of much more importance to have *a priori* knowledge of E_s/N_0 when employing FSK than when employing PSK, if linear metrics and equally spaced quantization intervals are going to be representative of the log likelihood probabilities.

For a given E_s/N_0 and Δ, the probability

$$p(w_{ij}^{(1)} = q \,|\, x_{ij} = 1), q = 0, \cdots, Q-1$$

can be determined from $F(y)$ in Eq. (28), and P_k in Eq. (26) is then determined as for binary PSK.

The above discussion applies to System A in Fig. 2. This implementation, namely the differencing of the analog envelope detection outputs before quantization, is easily implemented only for binary FSK. Since there is significant interest in MFSK because of its increased capacity (Ref. 5) we consider System B in Fig. 3, which is directly extendable to the M-ary case as shown in Fig. 8. With System B, each envelope detector is sampled and immediately quantized before any signal processing is carried out. In the binary case, the quantized outputs are linearly indexed over $0, \cdots, Q-1$, and differenced, with the result, designated as z_{ij} in Fig. 3, mapped into each of the two metrics $w_{ij}^{(1)}$ and $w_{ij}^{(0)}$. Under the assumption frequency f_1 was transmitted, hypothesis H_1, the PDF of r_1 and r_0 are again Rician and Rayleigh respectively.

To determine if $w_{ij}^{(1)}$ and $w_{ij}^{(0)}$ are representative of the log likelihood as is the case for the modems considered above, we must consider the likelihood ratio of the quantized received vector

$$z \triangleq (z_{ij}^{(1)}, z_{ij}^{(0)})$$

The log likelihood ratio is given by

$$\begin{aligned} LL(z) \triangleq{}& \ln P(z_{ij}^{(1)} \,|\, H_1) + \ln P(z_{ij}^{(0)} \,|\, H_1) \\ &- \ln P(z_{ij}^{(1)} \,|\, H_0) - \ln P(z_{ij}^{(0)} \,|\, H_0) \end{aligned} \tag{30}$$

since r_1 and r_0 are statistically independent random variables. Under H_1, the cumulative probability function of $y_{ij}^{(0)} \triangleq y$ is

$$F(y) = 1 - \exp(-y/2) \quad y \geqq 0 \tag{31}$$

and $y_{ij}^{(1)} \triangleq x$ has cumulative probability function

$$F(x) = 1 - Q(\lambda, \sqrt{x}), \qquad x \geqq 0 \tag{32}$$

where again

$$\lambda^2/2 = E_s/N_0 = ST_s/N_0$$

Since linear indexing is assumed as well as equally spaced quantization $z_{ij}^{(1)}$ and $z_{ij}^{(0)}$ can take on the values $0, \cdots, Q-1$, and z_{ij} can take on the values

$$-(Q-s), \cdots, -1, 0, 1, \cdots, Q-1$$

Computation has shown that the linear matrices

$$\left.\begin{aligned} w_{ij}^{(1)} &= z_{ij} \\ w_{ij}^{(0)} &= -z_{ij} \end{aligned}\right\} \tag{33}$$

are reasonably representative of the log likelihood. As shown above, the primary random variable in determining the performance of the Viterbi maximum likelihood sequence decoder is the difference of the log likelihood,

[2]Suggested by B. Levitt, Communications Systems Research Section, Jet Propulsion Laboratory.

namely $LL(z)$ in Eq. (30), which we desire to be represented by $w_{ij}^{(1)} - w_{ij}^{(0)}$.

Sample calculations are shown in Fig. 9. The difference of the log likelihood, $LL(z)$, is plotted against $w_{ij}^{(1)} - w_{ij}^{(0)}$ for $Q = 4$ quantization regions at the output of each envelope detector, and a quantization interval of $\Delta = 1.25$. The quantized outputs of each envelope detector are assigned the values 0, 1, 2, 3 for each of the four regions respectively. The difference can take on integral values over $[-3, 3]$. With the metric map in Eq. (33), this is identical to $w_{ij}^{(1)} - w_{ij}^{(0)}$. For each of the 16 possible values of the vector z, the difference of the log likelihoods versus $w_{ij}^{(1)} - w_{ij}^{(0)}$ is shown in Fig. 9 for $E_s/N_0 = 0$ dB and 1 dB. Multiple values appear, since values of $w_{ij}^{(1)} - w_{ij}^{(0)}$ can be obtained in several ways, each with its own value of $LL(z)$. The combination of $\Delta = 1.25$ and $E_s/N_0 = 0$ dB corresponds to the choice given by Eq. (29). It appears that this quantization procedure and choice of metrics is representative of $LL(z)$.

VI. Summary

A method is presented for determining an analytic approximation to the probability of error per bit for the Viterbi maximum likelihood sequence decoder which employs an arbitrary modem. The method is applied to the quantized binary PSK modem, and two implementations of the quantized binary FSK modem. Simple linear metrics are assumed and it is determined that they are quite representative of the log likelihood, the purpose being to demonstrate that implementation of a very simple metric is close to the optimum for a given Δ and E_s/N_0. If off-line decoding is to be performed, exact values of the metric could easily be employed, as used for example in the simulation carried out in Ref. 7.

References

1. Heller, J. A., and Jacobs, I. M., "Viterbi Decoding for Satellite and Space Communication," *IEEE Trans. on Communication Technology*, Vol. COM-19, No. 5, pp. 835–849, Oct. 1971.
2. Layland, J., "Performance of Short Constraint Length Convolutional Codes and a Heuristic Code-Construction Algorithm," in *The Deep Space Network*, Space Programs Summary 37-64, Vol. II, pp. 41–44, Jet Propulsion Laboratory, Pasadena, Calif., Aug. 31, 1970.
3. Viterbi, A. J., "Convolutional Codes and Their Performance in Communication Systems," *IEEE Trans. on Communication Technology*, Vol. COM-19, No. 5, pp. 751–772, Oct. 1971.
4. Huth, G. K., and Weber, C. L., "Minimum Weight Convolutional Code Words of Finite Length," *IEEE Trans. on Information Theory*, submitted.
5. Bar-David, I., and Butman, S., "Performance of Coded, Noncoherent, Hard-Decision MFSK Systems," in this volume of *The Deep Space Network Progress Report*.
6. Marcum, J. I., "A Statistical Theory of Target Detection by Pulsed Radar," *I.R.E. Trans. Info. Theory*, IT-6, Apr. 1960.
7. Richardson, R. J., Korgel, C. C., and Blizard, R. B., "Coding for Low Data Rate Noncoherent Channels," Report No. T-70-48813-001, Martin Marietta Aerospace Group, Denver, Colorado, Dec. 1970.

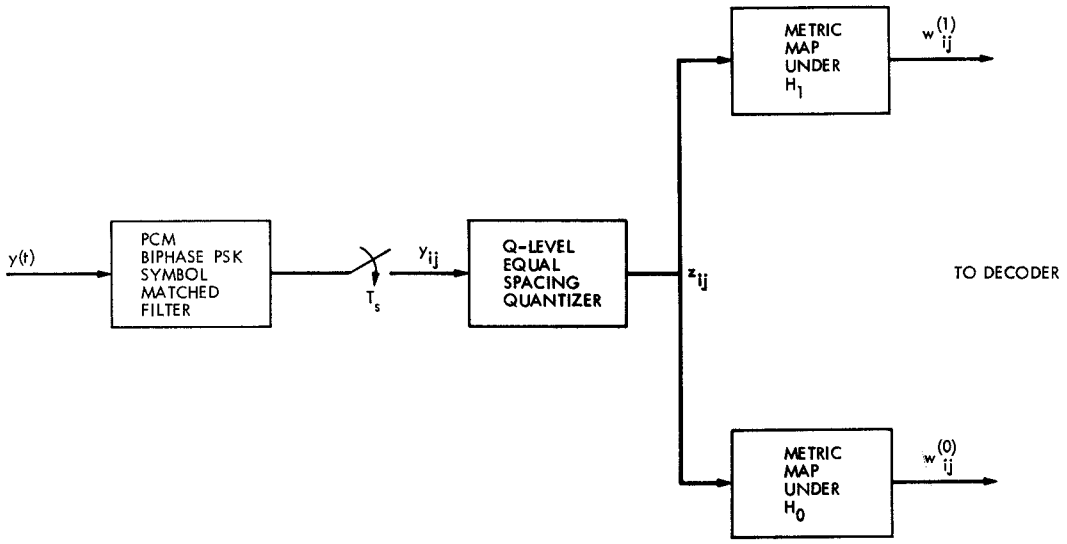

Fig. 1. PCM-PSK Biphase demodulator for the AWGN channel with Q-levels of quantization

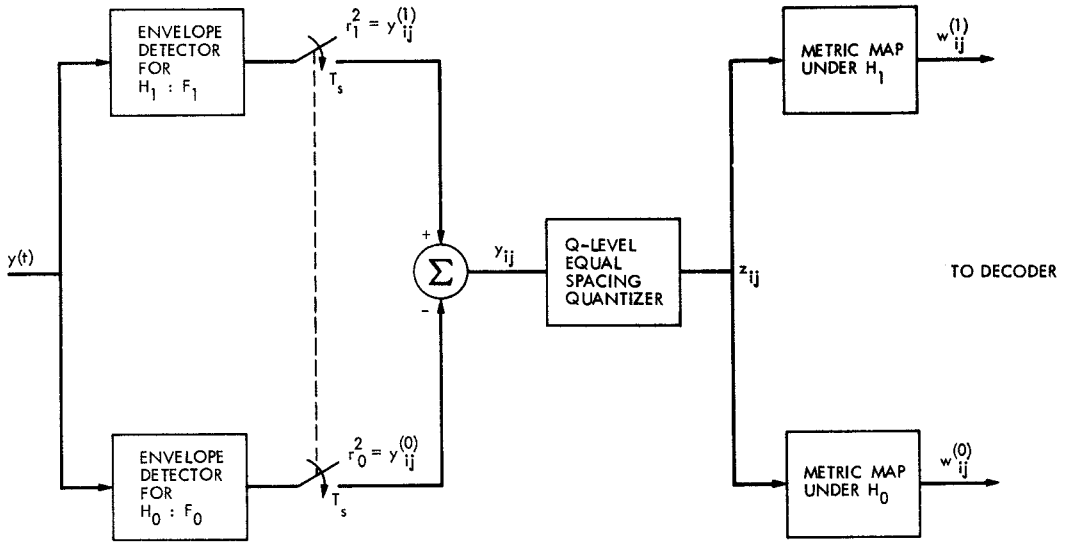

Fig. 2. PCM-binary FSK demodulator with Q-levels of quantization—System A

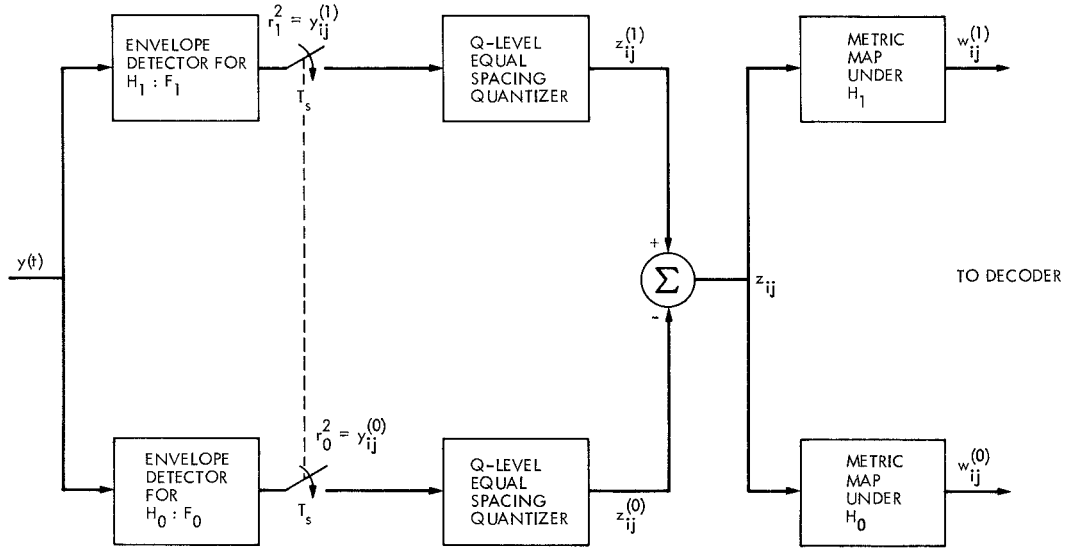

Fig. 3. PCM-binary FSK demodulator with Q-levels of quantization—System B

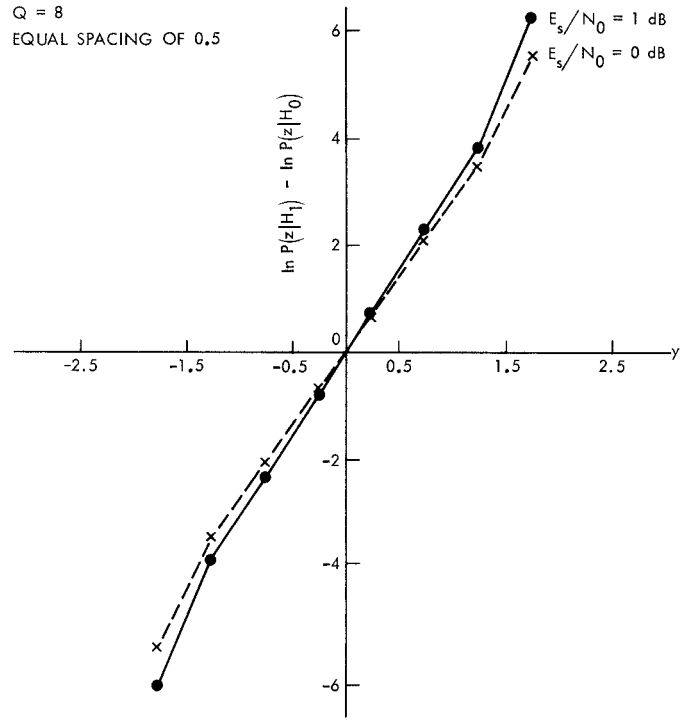

Fig. 4. Linearity of the difference of log likelihood with equally spaced quantization and the PSK modem

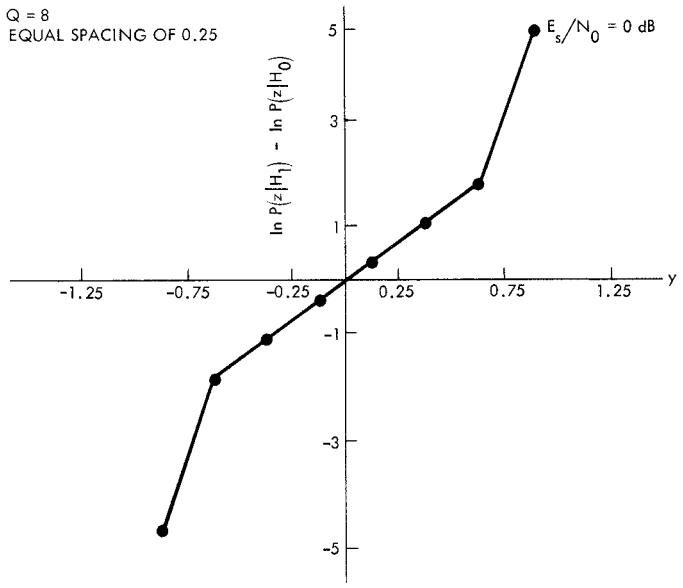

Fig. 5. Linearity of the difference of log likelihood with equally spaced quantization and the PSK modem

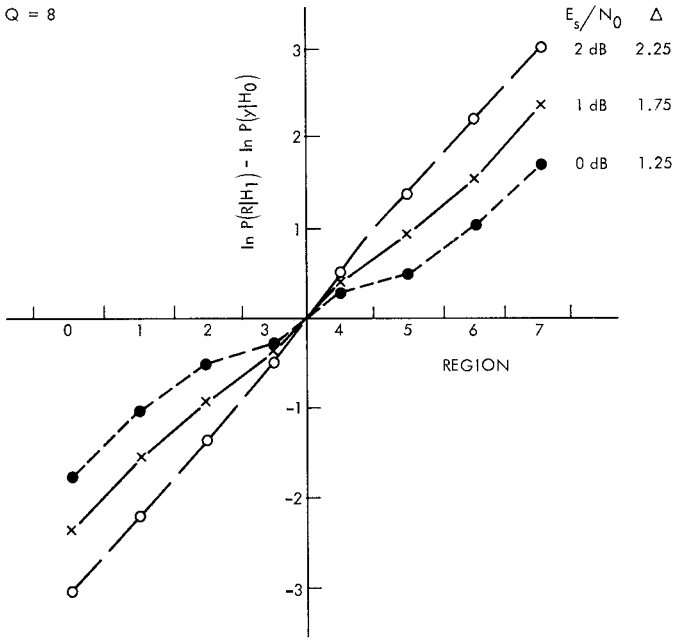

Fig. 6. Difference of log likelihoods of quantized outputs in binary FSK

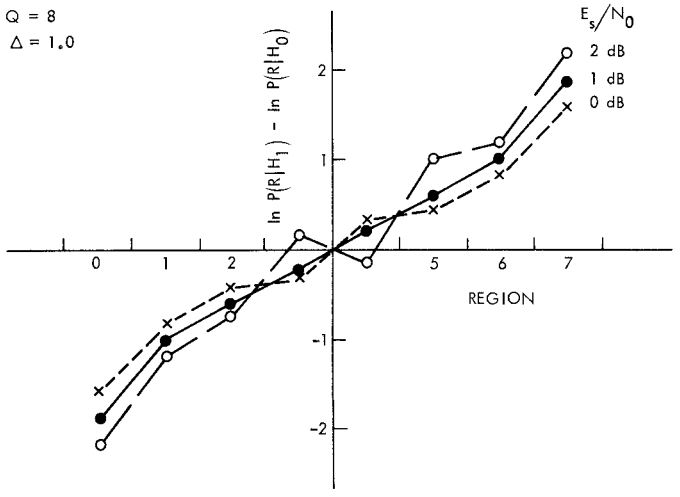

Fig. 7. Difference of log likelihoods of quantized outputs in binary FSK

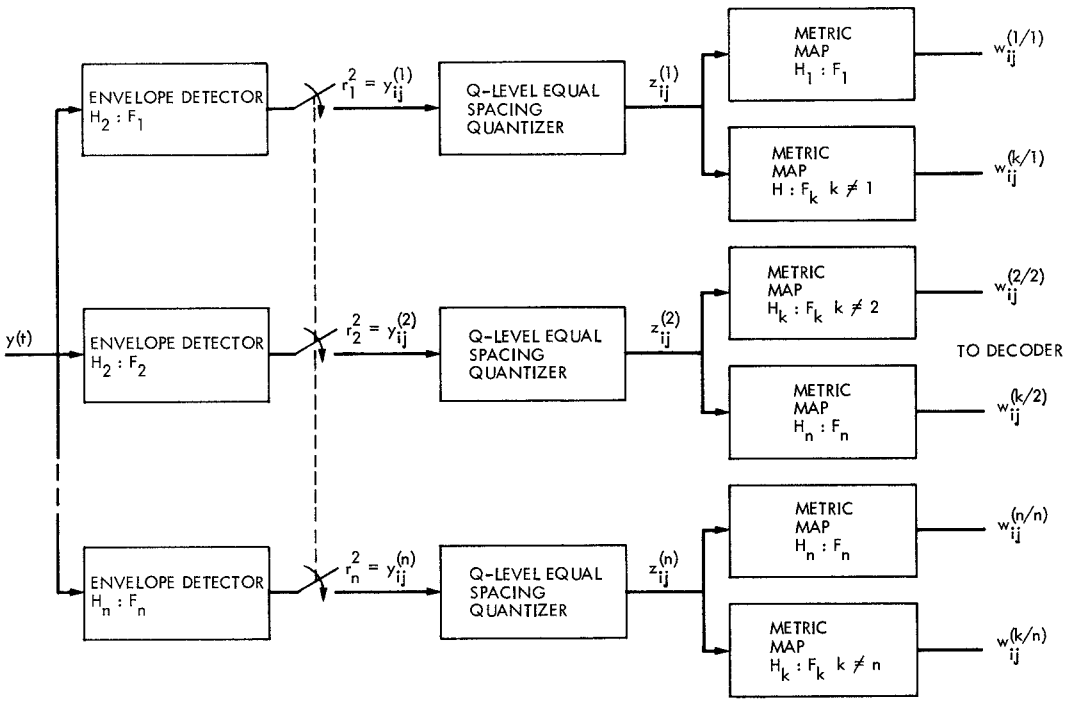

Fig. 8. PCM MFSK demodulator with Q-levels of quantization

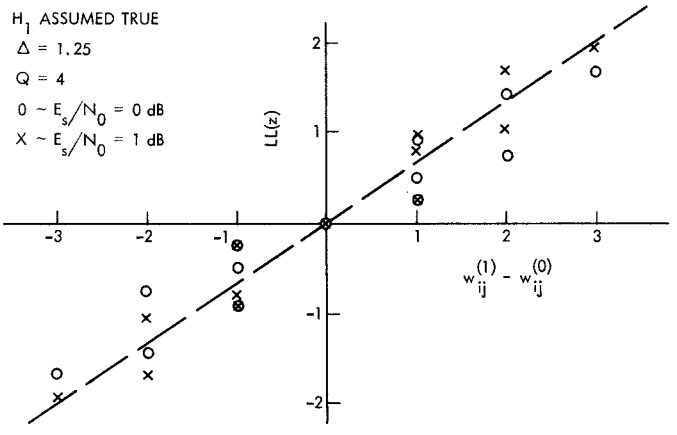

Fig. 9. Log likelihood ratio for System B, binary FSK, vs the difference of quantized, linearly indexed, envelope detector outputs